

Low-Voltage PLC Noise Modelling

F. Chelangat, T. J. O. Afullo

Abstract – This paper models the PLC impulsive noise using a linear superposition of univariate Gaussian distributions where the Bayes’ theorem is used to find the posterior probabilities. The Gaussian mixture is formulated using discrete latent variables and modelled using two, three and four components in order to evaluate the effect of the number of components (Q). The parameters of the Gaussian mixture are then estimated using the maximum likelihood technique and the expectation-maximization algorithm. Regression analysis is proposed in order to solve the issue of singularity which is often present when the maximum likelihood approach is employed. The model is then validated through measurements where the impulsive noise is categorized into low, medium and highly impulsive depending on the amplitude of the indoor PLC noise. It is observed that as the number of components increases the performance of the Gaussian mixture model also increases as depicted by the correlation coefficient and RMSE. The χ^2 test indicates that the proposed model provides a better fit as the PLC noise amplitude increases. In addition, the shape of the impulsive noise PDF becomes more defined with higher Q values. A singularity case is also examined where the Gaussian mixture model also provides a good approximation of the measured data. **Copyright © 2022 The Authors.**

Published by Praise Worthy Prize S.r.l. This article is open access published under the CC BY-NC-ND license (<http://creativecommons.org/licenses/by-nc-nd/3.0/>).

Keywords: Amplitude Distribution, Gaussian Mixture (GM), Impulsive Noise, Probability Density Function (PDF), EM Algorithm

Nomenclature

L	Lagrangian function
m_q	Mean of component q
m_{qp}	Updated mean
N	Sample size
N_q	Length of interval q
Q	Mixture component
R	Correlation coefficient
RMSE	Root Mean Square Error
y_g	Predicted PDF value
y_o	Measured PDF value
\bar{y}_g	Proposed PDF mean
\bar{y}_o	Measured PDF mean
y_n	Measured data point
Y_0	Initial data point
Y_n	Final data point
z_{nq}	Latent variable
χ^2	Chi-square Statistic
γ_{nq}	Posterior probability
λ	Lagrangian multiplier
π_q	Prior probability
π_{qp}	Updated mixture weight
σ_q	Standard deviation
σ_q^2	Variance
σ_{qp}	Updated variance
θ	Component parameters

Subscripts

q	Mixture component
qp	Updated value of component q

I. Introduction

Powerline communication (PLC), as a mode of data transmission, can be used to achieve data rates of up to 2Gbps [1], and is emerging in the broadband communication market as a strong competitor for indoor communication [2]. It provides an attractive alternative to the other communication systems due to its already existing infrastructure. However, like other communication systems, it is affected by noise which is a superposition of various heterogeneous components, particularly narrowband interference, coloured background noise and impulsive noise. The impulsive noise is further divided into periodic impulsive noise synchronous to the mains supply; periodic asynchronous to the mains supply; and asynchronous impulsive noise [3]-[6]. The most troublesome noise in broadband PLC is the impulsive noise, whose power can reach up to 50 dB above the thermal noise level [7]. The asynchronous impulsive noise, in particular, occurs randomly in bursts and has high power, leading to the obliteration of the communication signal [5], [6]. Thus, the development of a unified statistical model of this noise is a compelling task. To solve this problem, an adaptive model for the PLC noise needs to be employed. The Machine Learning

(ML) approach identifies regularities in data and has been employed in other fields such as [8], [9] to estimate the bit error rate and is classified into two main approaches: supervised and unsupervised learning. In the supervised learning approach, the input vectors and their corresponding target vectors comprise the training data while in the unsupervised learning only the input vectors are known and as such, the training data is composed of only the input vectors. The application of ML is still a new area of interest in PLC [10]. As such, [10] describes a general overview of its application including medium characterization, physical layer, media access layer, statistical modelling and grid diagnostics. A multi-layer perceptron model based on the ML method has also been employed to enhance the bit error rate performance of the PLC channel by significantly lowering the impulsive noise in [11]. In this work, unsupervised learning is employed such that for any measured PLC noise data, the training data set tunes the parameters of the model to suit the Probability Density Function (PDF) of the measured data. The Gaussian Mixture (GM) model is used to analyse the amplitude distribution of the PLC noise which is essential in predicting the amount of noise as seen by the receiver or the signal-to-noise ratio at the receiver. The effect of the number of components that constitute the GM on the impulsive noise amplitude distribution is examined. From the measurements carried out, the indoor impulsive noise is then categorized into low, medium and highly impulsive, where in each case a comparison is made between the proposed model and measurement results. In the proposed model the main contributions include:

1. Assessing the suitability and performance of the GM model with different number of components in modelling the PDF of the impulsive noise;
2. Regression analysis is proposed to solve the singularity problem present in the estimation of the GM model parameters that normally lead to the distribution density increasing to infinity;
3. The performance of the GM model under different indoor impulsive noise levels is evaluated;
4. A simple method of initializing the parameters in the EM algorithm is proposed.

The rest of the paper is organized as follows. In section II, an overview of previous studies on PLC noise is discussed while section III describes the measurement set-up and acquisition of measurement data. Section IV presents the GM model, parameter estimation and optimization. A brief description of the model calibration is covered in section V. The GM model is then applied to the measured data and the results are analysed in section VI. Finally, the conclusion and future work is presented in section VII.

II. Previous Work

One of the major advantages of PLC as a mode of data transmission is its ubiquitous infrastructure more so, in low-voltage environments. However, it comes at a cost as

it is characterized by heavy traffic in the wiring system resulting in time fluctuations of the PLC noise and is thus regarded as an unstable system with intermittent periodic impulsive noise [12]-[15]. Extensive measurements were carried out to investigate the noise contribution of different loads on the PLC channel in the 1-500 kHz and 2-12 MHz frequency bands in [16]. From the results obtained, the 1-500 kHz region was observed to have higher noise energy levels as compared to the 2-12 MHz frequency band. The total PLC noise as seen by the receiver is a summation of the background noise, narrowband interference and impulsive noise. Therefore, it is of primary importance to examine the properties of the PLC noise in order to design the most appropriate modulation and coding schemes for the PLC receiver system. Accordingly, various studies have been done in regards to the specific noise characteristics of the PLC noise based on the way in which the measurements were conducted. Hence, noise modelling can be classified into two approaches, namely: the frequency domain and the time-domain approach. The time domain approach captures the random characteristics of PLC noise at each frequency while the frequency-domain approach captures the average noise spectrum. Consequently, most PLC noise models are based on the time-domain approach.

The background noise is characterised by a very low power spectral density that varies with frequency caused by the summation of numerous noise sources with low power [3], [5]. In [17], the Rayleigh distribution has been employed in modelling the average noise amplitude distribution of the background noise at the receiver. This model is then extended to the Nakagami distribution which is a combination of multiple Rayleigh distributions since the background noise results from multiple noise sources. The closeness between the Rayleigh and the Nakagami distribution is measured by a parameter m such that at $m=1$, the Rayleigh and Nakagami distributions are equal [17]. At high frequencies, the unshielded electrical wires behave like antennas resulting in narrowband interference (NBI) of the transmitted signal by the amateur and commercial radio systems thereby degrading the performance of the PLC system.

As such, measurements capturing the NBI were performed by [18] in the 1-100 MHz frequency band in order to evaluate the NBI levels in the PLC network.

Moreover, in [19], the NBI model is developed using the 3D Markov chain for the low-voltage indoor broadband PLC network. The switching of rectifier diodes present in many electrical appliances results in periodic impulsive noise synchronous with the mains frequency while the switched power supplies are the main cause of periodic noise that occurs at a repetitive rate of between 50 kHz and 200 kHz. The cyclic features and the amplitude distributions of the PLC impulsive noise are modelled as a cyclostationary Gaussian process in [20] where it is expressed as the sum of simple and typical noise waveforms. This cyclostationary behaviour is also examined by [21] using the long-range dependence model where the PLC impulsive noise is

confirmed to exhibit self-similarity. Further investigations of the cyclostationary nature of the PLC noise were performed using the multi-fractal analysis in [13] where a more accurate method of obtaining the Hurst parameter is discussed. Both studies indicate that the PLC impulsive noise exhibits self-similarity [13], [21]. At high frequencies, the cyclostationary impulsive noise is seen to occur rapidly and at short time intervals in [22]. The asynchronous impulsive noise, on the contrary, occurs randomly and lasts for a few microseconds up to a few milliseconds. It mainly originates from switching transients in the PLC network.

In [23], the complementary the presence of cumulative density function method is used to detect impulsive noise in PLC. In this approach, the Middleton Class A and symmetric-alpha-stable models are used to determine the weights. Thereafter, the weighted sum of all the differences between the measured and the additive white Gaussian noise CCDF is used to determine the presence of impulsive noise. The characteristics of the various forms of impulsive noise have been investigated and the modelling is based on the impulse duration, inter-arrival time and the amplitude of the impulses. In [12], the likelihood of occurrence of single-impulse noise, background noise and bursty impulse noise is investigated. It was found that the bursty noise has the highest occurrence probability of at least 80% of the time, followed by background noise accounting for 15.57% while single-impulse events accounted for 2.8%.

The impulsive noise inter-arrival time and duration were also studied with the impulsive noise duration following the Weibull distribution. In terms of the inter-arrival time, single-impulse noise events followed the Exponential distribution while the bursty noise events were found to follow the Poisson distribution. Another property of the PLC noise is volatility clustering where the periods of low volatility are followed by periods of low volatility and the same case applies to periods of high volatility [4]. Therefore, the weighted average of the past squared residuals with reducing weights that never completely diminish is utilised to predict the subsequent variances [4]. In [24], the non-parametric kernel density technique is used to model the PLC noise amplitude distribution whereby the PDF of the measured data is estimated directly from the raw data without any prior assumptions about the particular structure of the underlying distribution since no fixed parameters are used to model the data. It is found that the kernel density provides a suitable estimate of the measured data.

Further research has been done in modelling the asynchronous impulsive noise, with recent surveys categorizing these models into those that have memory and those with no memory [6], [25]. The Markov-Middleton and Markov-Gaussian models belong to the model category with memory [6], [25]. The popular models with no memory include the Middleton Class A and Bernoulli-Gaussian models, which are forms of the Gaussian Mixture (GM) model. Symmetric-alpha-stable distribution is increasingly becoming popular and has

recently been employed to model the heavy tails exhibited by the PLC impulsive noise due to their heavy-tailed and skewness characteristic [26], [27]. Even so, the symmetric-alpha-stable distribution is described only by their characteristic equations as they do not have a useful analytical and closed form for its PDF [12]. A comparative study is performed on the modelling of impulsive noise amplitude in [1], where the Student's *t*-distribution is proposed. In the Middleton Class A model, the PLC impulsive noise is determined by summing several Gaussian distributions with zero mean and different variances which are Poisson distributed [28]. It has been applied in [29], to determine the channel capacity as well as characterise the performance of the broadband PLC through the detection of binary phase shift keying symbols. On the other hand, the BG model assumes two states- impulsive and impulse-free- which can be seen as a two-state representation of the Middleton Class A model but with the weights, Bernoulli distributed [6], [25]. The GM models are widely used due to their simplicity. However, they do not factor in the bursty nature of the impulsive noise, as the noise, in this case, is assumed to be independent and identically distributed (i.i.d.). This shortfall can be addressed using multi-carrier modulation, whereby the time domain impulse noise is spread by discrete Fourier transform on all the sub-carriers in the frequency domain such that the form in which the noise occurred either randomly or in bursts becomes irrelevant [30]. Mixing of the different components of the Gaussian Mixture (GM) has been achieved using statistical distributions such as Bernoulli and the Poisson distribution which increases the complexity of the models. The Middleton Class A model, for example, requires the evaluation of the impulsive noise to power ratio as well as identifying the number of impulsive noise components which is a challenging task.

There are several studies on the impulsive noise PDF focused on modelling the tail of the distribution and is assumed that the means of the Gaussian mixtures are zero as seen in [31], [32]. Moreover, the number of components in the Middleton Class A is also truncated at three which is seen to be sufficient enough in modelling the PLC impulsive noise [25]. The impulsive noise affecting each sub-carrier of the orthogonal frequency division multiplexing system which employs binary phase-shift keying is modelled using the generalised Gaussian model [33]. However, in [34], the generalised Gaussian model was extended to model the bi-dimensional constellations where it was observed to lead to significant errors, particularly in multi-modal measurement distributions. From previous studies, the PLC noise is confirmed to exhibit self-similarity whereby if the observed sample is divided into different clusters, then each cluster would possess the same statistical properties as the whole data set [21]. This self-similarity property is applied in the proposed GM model, such that the mean and variance of the measured PLC noise for the different clusters are applied to the whole sample. As such, each component is assumed to be Gaussian

distributed and the resulting noise amplitude distribution is also Gaussian. The volatility clustering characteristic of the PLC noise presented in [4], has also been exploited in the proposed model. The Gaussian mixture is a heteroscedastic model since the mean and variance are functions of the measured data. Consequently, the mean and variance of each cluster vary depending on whether the cluster captures a period of high volatility or a period of low volatility. Although the amplitude distribution of the PLC noise in [24], is derived solely from the measured data with no prior assumptions as regards the characteristic nature of the measured data, the effectiveness of the model is based on the determination of the optimum bandwidth. Accordingly, several iterations are performed to obtain the optimal model, on which depending on the errors obtained from the goodness of fit test, the bandwidth is adjusted. The proposed GM model provides a simple straightforward way of determining the amplitude distribution of the PLC noise where the unsupervised learning approach is employed to find clusters that exhibit comparable properties within the measured noise data. In [35], the GM model is applied in modelling the Bit Error Rate (BER) of the PLC channel. The BER is formulated from the impulsive noise PDF where the parameters of the model are acquired through soft learning of the observed samples. The parameters of the GM are estimated through the maximum likelihood estimate and optimised using the expectation-maximization algorithm. The optimum number of components of the GM model is obtained from the Mutual Information theory framework and the model is seen to provide a fair estimate for the measured data.

In this work, further considerations are made on the PDF modelling of impulsive noise using the GM model proposed in [35]. Different number of components are used to formulate the Gaussian mixture and the performance of each GM mixture model is investigated. In addition, the effect of singularity where the EM algorithm does not converge on the GM model PDF is examined. A simple procedure of initialising the parameters of the GM model is also proposed. The PLC impulsive noise is assumed to be a linear superposition of the univariate Gaussian distributions. The data is divided into subsets for which the mean and the variance of each subset are determined, and then applied to the whole data set. Parameters of the GM are then derived from the maximum likelihood estimation technique where the Bayesian theorem is used to determine the posterior probabilities which are referred to as responsibilities.

These are then used to compute the 'new' parameters of the GM model namely: the mixing weights, means, and variance. In order to find the optimum parameters, the Expectation Maximization (EM) algorithm is employed. Thereafter, regression analysis is performed to determine the accuracy of the proposed model. It also solves the issue of singularities in the likelihood function where a Gaussian component collapses to a single data point.

III. Measurement Set-Up

Due to the complex nature of the PLC noise, the models developed, both parametric and non-parametric are mostly based on measurements. Therefore, to provide plausible descriptions of the acquired data sample, a rigorous measurement campaign of PLC noise need to be conducted. In this work, comprehensive noise measurement was carried out using a higher resolution Rigol DS2202A Digital Storage Oscilloscope (DSO) connected via a coupling circuit to the powerline network. The measurement setup is shown in Fig. 1.

The oscilloscope is capable of capturing 14 million samples whereby the sampling rate is set at 1 Giga samples/s, thus exploiting the maximum storage capacity of the oscilloscope as the resulting window length is 0.014 seconds. The measured data is then transferred to the computer for processing and storage. A differential mode coupler is used to isolate the high voltage mains supply ensuring the safety of the equipment as well as filtering out the low-frequency signals. The coupler comprises a 1:1 broadband transformer, series capacitors, transient voltage suppressors and Zener diodes. The series capacitance together with the leakage inductance of the transformer create a series resonant coupling circuit. Investigations have been done regarding the effect of the coupling circuits on the PLC impulsive noise [36], where the results indicate that as the PLC noise passes through the coupling circuit, it excites points of resonance in the coupler. Consequently, this results in resonance which introduces ringing to the impulse noise.

The ringing effect then distorts the impulse duration, inter-arrival time and amplitude of the impulse signal [36]. Further investigations on the effect of the coupler on impulsive noise are discussed in [36]. In this work, the effect of the coupling circuit is not considered as the focus is on the PLC noise in general as seen by the receiver. In order to examine the contribution of different loads present in typical PLC environments to the PLC noise, measurements were carried out in different locations in the 1-30 MHz frequency band. Four locations are considered in this study namely Computer laboratory (Computer Lab), Post-graduate office, Apartment and Machines Laboratory (Machines Lab).

In the Computer Lab, the electric loads connected include an air-conditioner, sixty computers and fluorescent lights.

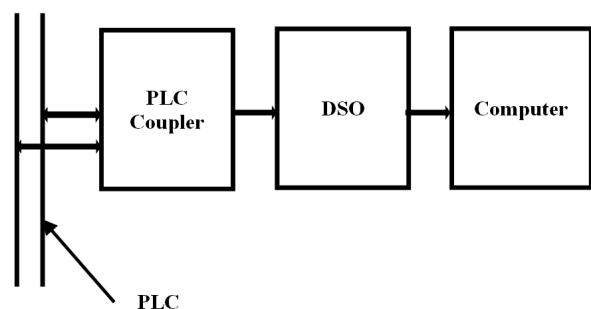


Fig. 1. Measurement Set-up

The measurements were performed between 2:00 pm to 5:00 pm during which all the stations were occupied as the students performed their practicals. The electrical devices connected to the Post-graduate powerline network include laptop and desktop computers, fluorescent lights, mobile phones, air-conditioning units, an electric kettle and a heavy-duty printer (Konica Minolta C364 model) that serves all the post-graduate students in the Northern and Southern Electrical buildings at the University of KwaZulu-Natal. The measurement results were obtained during the day when the office is preoccupied between 8:00 am and 5:00 pm.

As for the Apartment, the loads connected to the powerline network include light dimmers, washing machine, television set, fluorescent lights, electric kettle, vacuum cleaner, electric cooker, microwave oven, juice blender, iron box and security lights. In this location, measurement was conducted between 6:00 pm to 9:00 pm whereby most of the electric appliances in the house are switched on and active.

The Machines Lab measurement campaign was carried out between 2:00 pm and 5:00 pm, during which the students undertook their practicals. The Machines Lab contains 9 workstations in which each of the stations comprises an ac motor, dc generator, adjustable speed drive, variac with an in-built rectifier and a variable resistor of up to 450 Ω .

Other loads in the Machines Lab include fluorescent lights and air-conditioners. All of the scenarios are located at the University of KwaZulu-Natal except for the Apartment. Sample measurement noise results from the different locations are shown in Figs. 2.

The PLC noise, as observed from the sample noise measurements in Figs. 2, is difficult to characterize and model through pure mathematical derivation. Thus, the parameters for the statistical models are derived from the distribution into certain PDFs that fully describe the overall noise characteristics.

IV. Proposed Model

In the proposed model, impulsive noise is assumed to be i.i.d. random variables whose PDF is generated from the weighted sum of a linear superposition of Gaussian distributions (components) with the mixing probabilities summing up to one. Thus, at any given time constant, the noise is a random variable. The discrete-latent variable model is used to formulate the GM whereby for each observed data point y_n where $n=1,2,\dots,N$, there is a corresponding latent variable z_{nq} , that indicates whether the q_{th} mixture component generated that data point for $q=1,2,\dots,Q$ [37]. Thus, the data point y_n can only be generated by the q_{th} mixture component given by [37]:

$$p(y_n | z_{nq} = 1) = N(y_n | m_q, \sigma_q) \quad (1)$$

where $N(y_n|m_q,\sigma_q)$ is the q_{th} Gaussian density defined as [38], [39]:

$$N(y_n | m_q, \sigma_q) = \frac{1}{(2\pi)^{\frac{1}{2}} \sigma_q} \exp\left[-\frac{(y_n - m_q)^2}{2\sigma_q^2}\right] \quad (2)$$

and m_q, σ_q are the mean and standard deviation. Since the latent variable z_{nq} is unknown, a prior distribution is placed such that:

$$p(z_{nq} = 1) = \pi_q \quad (3)$$

where:

$$\pi_q = \begin{cases} 1, & \text{if } y_n \in N(y_n | m_q, \sigma_q) \\ 0, & \text{otherwise} \end{cases}$$

$$\sum_{q=1}^Q \pi_q = 1 \quad (4)$$

Ancestral sampling technique is then used to generate the value of y_n by computing the joint distribution of the latent variable $p(z_{nq}=1)$, and the conditional distribution $p(y_n|z_{nq}=1)$ to obtain [37]:

$$p(y_n) = \pi_q N(y_n | m_q, \sigma_q) \quad (5)$$

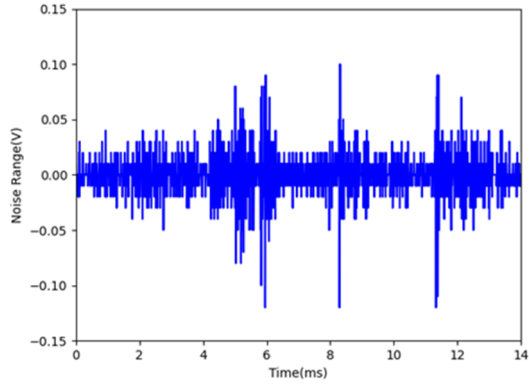
The sum of the joint distribution over all possible states of z_{nq} results in the PDF of the Gaussian mixture for data point y_n such that at any given time constant, the noise is a random variable whose PDF is defined as:

$$p(y_n | \theta) = \sum_{q=1}^Q \pi_q N(y_n | m_q, \sigma_q) \quad (6)$$

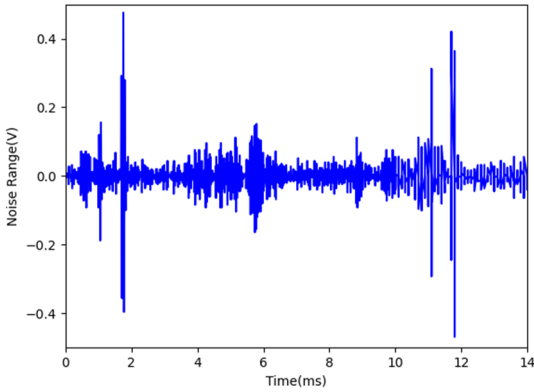
where $\theta = \{m_q, \sigma_q, \pi_q; q=1, 2, \dots, Q\}$ is a collection of all parameters of the model. The corresponding posterior probability (responsibility) of z_{nq} given y_n can be determined using Bayes' theorem as [38]:

$$\begin{aligned} \gamma_{nq} &= p(z_{nq} = 1 | y_n) = \\ &= \frac{p(z_{nq} = 1) p(y_n | z_{nq} = 1)}{\sum_{j=1}^Q p(z_{nj} = 1) p(y_n | z_{nj} = 1)} \\ &= \frac{\pi_q N(y_n | m_q, \sigma_q)}{\sum_{j=1}^Q \pi_j N(y_n | m_j, \sigma_j)} \end{aligned} \quad (7)$$

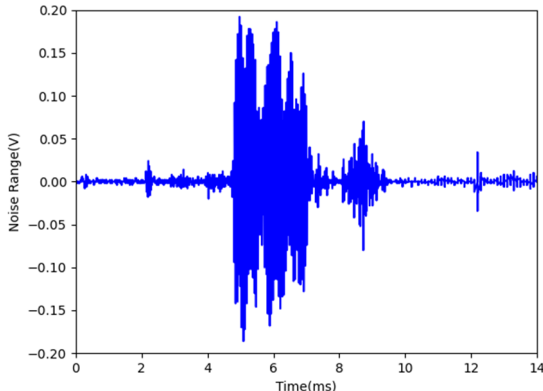
Equation (7), gives the probability that the q_{th} mixture component generated the n_{th} data point. Thus, π_q denotes the prior probability and defines the mixing weights in the GM model while γ_{nq} denotes the posterior probability once y_n has been observed.



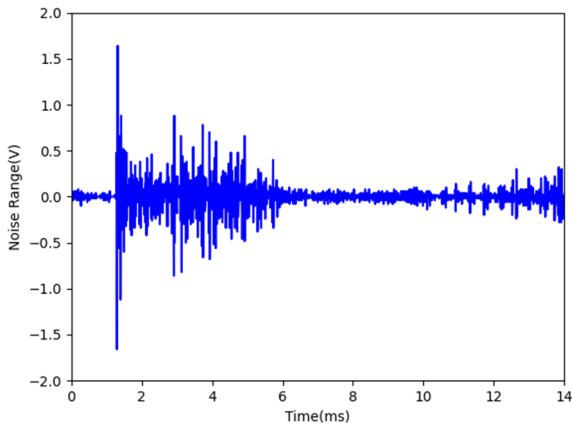
(a) Computer Lab



(b) Post-Graduate Office



(c) Apartment



(d) Machines Lab

Figs. 2. Measured Noise Samples

IV.1. Parameter Estimation

In order to estimate the parameters of the GM, the maximum likelihood technique is employed where these parameters are derived from the measured impulsive noise data. Thus, if N is the total number of observations for a given data set $Y=y_1, y_2, \dots, y_n$, the likelihood function of the Gaussian mixture is given as:

$$p(Y | \theta) = \prod_{n=1}^N p(y_n | \theta) \quad (8)$$

where $p(y_n|\theta)$ refers to the Gaussian density of every individual likelihood. Equation (8) can be simplified by taking the log of the likelihood function to obtain:

$$\begin{aligned} \log p(Y | \theta) &= \sum_{n=1}^N \log p(y_n | \theta) \\ &= \sum_{n=1}^N \log \sum_{q=1}^Q \pi_q N(y_n | m_q, \sigma_q) \end{aligned} \quad (9)$$

The derivative of equation (9) with respect to m_q is obtained as [37]:

$$\frac{\partial \log p(Y | \theta)}{\partial m_q} = \sum_{n=1}^N \frac{1}{p(y_n | \theta)} \frac{\partial p(y_n | \theta)}{\partial m_q} \quad (10)$$

$p(y_n|\theta)$ in Equation (10), is given as:

$$p(y_n | \theta) = \sum_{j=1}^Q \pi_j N(y_n | m_j, \sigma_j) \quad (11)$$

It follows that only the q th mixture component depends on m_q and therefore:

$$\begin{aligned} \frac{\partial p(y_n | \theta)}{\partial m_q} &= \pi_q \frac{\partial N(y_n | m_q, \sigma_q)}{\partial m_q} \\ &= \frac{\pi_q}{(2\pi)^{\frac{1}{2}} \sigma_q} \frac{\partial \exp\left(-\frac{(y_n - m_q)^2}{2\sigma_q^2}\right)}{\partial m_q} \end{aligned} \quad (12a)$$

Applying Chain rule to (12a):

$$\begin{aligned} \frac{\partial p(y_n | \theta)}{\partial m_q} &= (y_n - m_q)(\sigma_q)^{-1} \times \\ &\times \frac{\pi_q}{(2\pi)^{\frac{1}{2}} \sigma_q} \exp\left(-\frac{(y_n - m_q)^2}{2\sigma_q^2}\right) \\ &= (y_n - m_q)(\sigma_q)^{-1} \pi_q N(y_n | m_q, \sigma_q) \end{aligned} \quad (12b)$$

Substituting (11) and (12b) to (10):

$$\begin{aligned} \frac{\partial \log p(Y | \theta)}{\partial m_q} &= \\ &= \sum_{n=1}^N (y_n - m_q) (\sigma_q)^{-1} \frac{\pi_q N(y_n | m_q, \sigma_q)}{\sum_{j=1}^Q \pi_j N(y_n | m_j, \sigma_j)} \quad (13) \\ &= \sum_{n=1}^N \gamma_{nq} (y_n - m_q) \sigma_q^{-1} \end{aligned}$$

where γ_{nq} has been defined in equation (7). The updated mean m_{qp} is then determined by setting the derivative in (13) to zero to obtain:

$$m_{qp} = \frac{1}{N_q} \sum_{n=1}^N \gamma_{nq} y_n \quad (14)$$

where N_q is the total number of points assigned to the q th mixture component and is given by:

$$N_q = \sum_{n=1}^N \gamma_{nq} \quad (15)$$

Similarly, the derivatives of (9) with respect to σ_q^2 and π_q are obtained as [37], [38]:

$$\frac{\partial \log p(Y | \theta)}{\partial \sigma_q} = \sum_{n=1}^N \frac{1}{p(y_n | \theta)} \frac{\partial p(y_n | \theta)}{\partial \sigma_q} \quad (16)$$

$$\frac{\partial \log p(Y | \theta)}{\partial \pi_q} = \sum_{n=1}^N \frac{1}{p(y_n | \theta)} \frac{\partial p(y_n | \theta)}{\partial \pi_q} \quad (17)$$

The corresponding updated variance σ_{qp} is then given by:

$$\sigma_{qp} = \frac{1}{N_q} \sum_{n=1}^N \gamma_{nq} (y_n - m_q)^2 \quad (18)$$

In order to compute the partial derivative of the mixture weight π_q , the constraint that all mixture weights need to sum up to 1, given in (4), is accounted for by using the Lagrangian multiplier. The corresponding Lagrangian is given as [35], [37], [38]:

$$L = \log p(Y | \theta) + \lambda \left(\sum_{q=1}^Q \pi_q - 1 \right) \quad (19)$$

The partial derivatives with respect to π_q and Lagrange multiplier λ are then obtained as:

$$\frac{\partial L}{\partial \pi_q} = \sum_{n=1}^N \frac{N(y_n | m_q, \sigma_q)}{\sum_{j=1}^Q \pi_j N(y_n | m_j, \sigma_j)} + \lambda = \frac{N_q}{\pi_q} + \lambda \quad (20)$$

$$\frac{\partial L}{\partial \lambda} = \sum_{q=1}^Q \pi_q - 1 \quad (21)$$

Setting the partial derivatives of equations (20) and (21) to zero and solving for π_q the updated mixture weight π_{qp} is obtained as:

$$\pi_{qp} = \frac{N_q}{N} \quad (22)$$

The EM algorithm aims at maximizing the likelihood function with respect to the means, variances and mixing coefficients of the components. It achieves this by iteratively refining the initial parameters alternating between updating the cluster assignments and parameter estimates. With each iteration, the mean of each component Gaussian distribution moves towards the mean of the data in the cluster. For the proposed model, the EM algorithm consists of the following steps [35], [38]:

1. Initialize m_q , σ_q and π_q , then evaluate the initial value of the log-likelihood;
2. Expectation step (E-step): Compute the responsibilities, using the current parameters:

$$\gamma_{nq} = \frac{\pi_q N(y_n | m_q, \sigma_q)}{\sum_{j=1}^Q \pi_j N(y_n | m_j, \sigma_j)} \quad (23)$$

3. Maximization step (M-step): Re-evaluate the parameters using the current responsibilities to obtain the updated mean, variance and mixing weight represented by m_{qp} , σ_{qp} and π_{qp} respectively:

$$m_{qp} = \frac{1}{N_q} \sum_{n=1}^N \gamma_{nq} y_n \quad (24)$$

$$\sigma_{qp} = \frac{1}{N_q} \sum_{n=1}^N \gamma_{nq} (y_n - m_q)^2 \quad (25)$$

$$\pi_{qp} = \frac{N_q}{N} \quad (26)$$

where:

$$N_q = \sum_{n=1}^N \gamma_{nq} \quad (27)$$

4. Evaluate the log-likelihood:

$$\log p(Y|\theta) = \sum_{n=1}^N \log \sum_{q=1}^Q \pi_q N(y_n | m_q, \sigma_q) \quad (28)$$

5. Check for convergence of either the log-likelihood or the parameters. If the convergence criterion is not satisfied, return to step 2.

IV.2. Parameter Initialization

The EM algorithm discussed in the previous section consists of the E-step and the M-step. In the E-step, the posterior probabilities are evaluated using the initial values of the parameters. Thereafter, the posterior probabilities are used to re-estimate the updated (new) means, variances and mixing weights. Although the maximum likelihood solution suffers from identifiability, whereby a Q -component mixture will have a total of Q -equivalent solutions for a particular maximum likelihood solution that corresponds to the $Q!$ methods in which the Q -sets of parameters can be assigned to the Q -components, this issue is irrelevant if the purpose is to find a good density model since each of the equivalent solutions is as good as the others [38]. The parameters of the proposed model are derived from the independent and identically distributed random variables of the measured time-domain sequence of noise samples in the low-voltage indoor environment. As such, at each time instant t , there is an impulse noise variable y_n , with a specific amplitude. The time domain amplitude distribution of the measured data is shown in Fig. 3 and the corresponding sample sequence series with two intervals is illustrated in Fig. 4. As such, the observation window is divided into Q intervals of equal length such that:

$$N_q = \frac{Y_n - Y_o}{Q} \quad (29)$$

where N_q is the length of the q_{th} interval and represents the total number of samples in the q_{th} interval, $Y_N=1400$ and $Y_o=0$ from Fig. 4. Accordingly, each interval provides the parameters of the components of the Gaussian mixture.

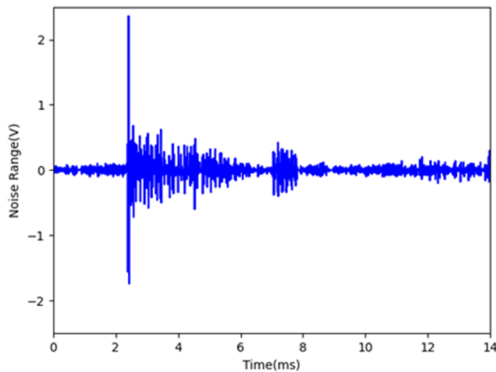


Fig. 3. Noise Amplitude Distribution

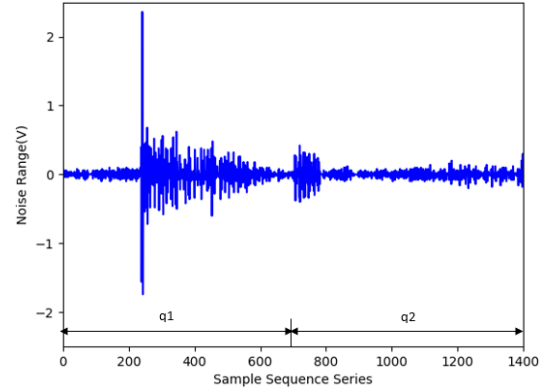


Fig. 4. Sample Sequence Series

Therefore, the probability that the average noise level in the observation window is in the k_{th} cluster is then given by:

$$\pi_q = \frac{N_q}{N} \quad (30)$$

In the proposed model, initialization of these parameters consists of the following steps:

1. Divide the data into Q clusters;
2. Compute the ratio of the number of points in each cluster to the total number of samples. This gives the initial mixing weights;
3. Determine the mean and variance of each cluster. This gives the means and variances for the individual components of the Gaussian mixture;
4. Compute the Gaussian distributions for the whole data set using the means and variances found in step 3.

IV.3. Selection of Optimum Parameters

From the EM algorithm, the optimum parameters are found by checking the convergence of either the log-likelihood function or parameters. However, in some cases, the algorithm may not converge due to singularities of the likelihood function which may occur when the maximum likelihood method is applied to estimate the parameters. This occurs when a data point has a value that is exactly equal to the mean of one of the component distributions. Thus, from (6), the n_{th} data point will contribute to a term in the likelihood function of the form:

$$N(y_n | m_q, \sigma_q) = \frac{1}{(2\pi)^{\frac{1}{2}} \sigma_q} \quad (31)$$

Hence, as $\sigma_q \rightarrow 0$, the likelihood function tends to infinity and the same case applies to the log-likelihood function. A Gaussian mixture has a minimum of two components. As such, if one of the component distributions collapses to a particular data point, the other component with a finite variance assigns a finite

probability to all the data points thereby contributing an ever-increasing additive value to the log-likelihood. In order to solve this problem, regression analysis is performed to determine the iteration whose parameters best describe the measured data.

V. Model Calibration

The Pearson’s parametric correlation (R) test is performed in this work to measure the degree of dependency between the GM model and the measured data. The Root Mean Square Error (RMSE) test and the Chi-Square statistic (χ^2) are also used to analyse the goodness-of-fit of the GM model based on their residuals. Equations (33), (34) and (35) define R , RMSE and χ^2 respectively as [12], [24]:

$$R = \frac{\sum_{n=1}^N (y_o - \bar{y}_o)(y_g - \bar{y}_g)}{\sqrt{\sum_{n=1}^N (y_o - \bar{y}_o)^2 (y_g - \bar{y}_g)^2}} \quad (32)$$

$$RMSE = \sqrt{\frac{\sum_{n=1}^N (y_o - y_g)^2}{N}} \quad (33)$$

$$\chi^2 = \sum_{n=1}^N \frac{(y_o - y_g)^2}{y_g} \quad (34)$$

where y_o is the measured value, y_g is the proposed model value, \bar{y}_o and \bar{y}_g are the means of the measured and the proposed model value while N is the measurement sample size. The objective of the Chi-Square test in this work is to evaluate the deviation between the expected model results from measurement. Thus, the null hypothesis states that the measured data follows the GM distribution while the alternative hypothesis states that the measured data does not follow the proposed GM distribution. The significance level is set at 5% and hence a p-value <0.05 indicates that the null hypothesis is rejected and therefore conclude that the measured data does not follow the proposed GM distribution.

Otherwise, if the p-value >0.05 the null hypothesis is accepted and conclude that the measured data is consistent with the proposed model distribution results.

VI. Results and Discussion

The impulse noise amplitude, width and inter-arrival time are the major properties of impulsive noise. The proposed model seeks to extend the knowledge of the PLC noise where the impulsive noise amplitude characteristic is investigated. The measured data is categorized into three categories depending on the peak-

to-peak(pp) amplitude voltage as low, medium and highly impulsive. The low, medium and highly impulsive noise ranges are $0 \leq y \leq 0.25V_{pp}$, $0.25 < y \leq 2V_{pp}$ and $y > 2V_{pp}$ respectively. For each category, the PDF is modelled using a GM composed of two components ($q=2$), three components ($q=3$) and four components ($q=4$). The performance of each GM is analysed using the correlation coefficient, RMSE and the χ^2 statistic for each measured data.

In Fig. 5, it is observed that as the number of Gaussian mixture components increases, the peak of the curve increases as well. The peak of the $q=3$ model is also seen to be close to the peak of the measured data. In addition, from Table I the $q=4$ Gaussian mixture shows a good correlation with the measured data where the correlation coefficient values range between 0.9857 to 0.9897 with the highest correlation observed for the four component GM model. Thus, there is a strong correlation between the predicted and the measured data as all the values are above 0.98. It can also be seen from Table I that the four-component GM model performs better than the other two models with an RMSE of 0.1716 as compared to 0.1842 and 0.1821 for the two and three-component GM models in measurement 1. From Fig.6, it is observed that at $q=4$ and $q=3$ the shape of the predicted density follows closely the measured data. For $q=2$, there is no notch between the two peaks as is the case with the three and four-component GM models. From Table I, measurement 2, the two-component model has a lower correlation as compared to the other models with a value of 0.9761. In terms of accuracy, the RMSE values range from 0.1653 to 0.2463 where the $q=4$ model has the least RMSE value. All the models, in this case, have a high correlation to the measured data. In both cases, the three component GM model correlation coefficient and the RMSE values fall in between $q=2$ and $q=4$.

TABLE I
LOW IMPULSIVE

Model	Computer Lab					
	Measurement 1			Measurement 2		
	q=2	q=3	q=4	q=2	q=3	q=4
R	0.9857	0.9860	0.9897	0.9761	0.9801	0.9893
RMSE	0.1842	0.1821	0.1716	0.2463	0.2446	0.1653

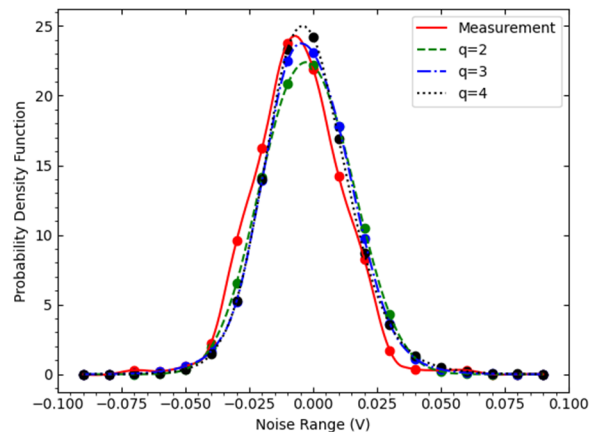


Fig. 5. Low Impulsive: Measurement 1

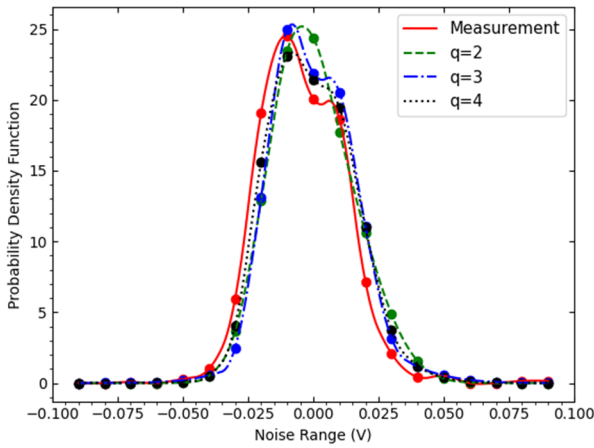


Fig. 6. Low Impulsive: Measurement 2

From Figs. 5 and 6, the measured PDF for the Computer Lab has no outliers caused by high amplitude impulse noise. This is because the computers in this location use switched mode power supplies that have been confirmed to produce impulsive noise of low amplitude as confirmed in [17]. As such, any increased amplitude in the Computer Lab is caused by fluorescent lights that have been confirmed to produce higher impulse noise levels [17], [40]. For the medium impulsive noise category, the GM models at the $q=2$, $q=3$ and $q=4$ overlap as shown in Fig. 7 and Fig. 8. In this case, the likelihood function for the different Q-component GM models are seen to result in the same density distribution. Moreover, the correlation coefficients are the same for $q=2$ where $R=0.9718$ and $q=24$ having $R=0.9726$ for the two measurement data as summarized in Table II. The correlation coefficient varies slightly at $q=3$. This can be attributed to the occurrence of impulsive noise of similar amplitude levels as the measurement is taken in the same location.

However, the RMSE values vary with the RMSE values for measurement 1 ranging between 0.1875 and 0.1849 while for measurement 2 the values are between 0.1935 and 0.1908. The correlation coefficients and the RMSE values for the medium impulsive noise are shown in Table II.

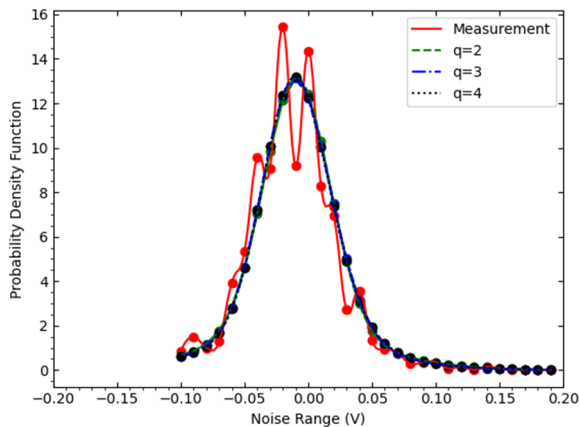


Fig. 7. Medium Impulsive: Measurement 1

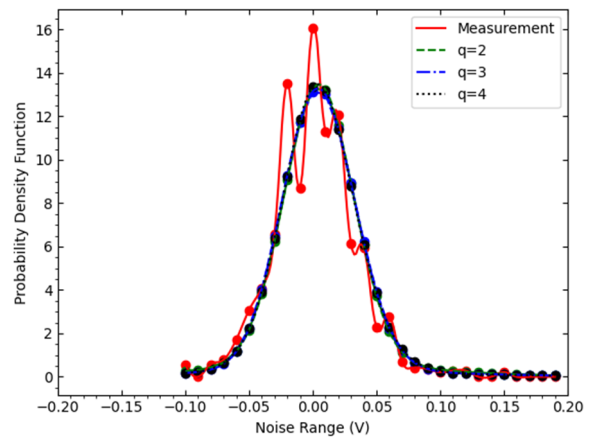


Fig. 8. Medium Impulsive: Measurement 2

TABLE II
MEDIUM IMPULSIVE

Post-Graduate Office						
	Measurement 1			Measurement 2		
Model	q=2	q=3	q=4	q=2	q=3	q=4
R	0.9718	0.9725	0.9726	0.9718	0.9723	0.9726
RMSE	0.1875	0.1852	0.1849	0.1935	0.1918	0.1908
Apartment						
	Measurement 1					
Model	q=2	q=3	q=4			
R	0.9877	0.9828	0.9871			
RMSE	0.2875	0.3400	0.2950			

Fig. 9 presents the density distribution of the impulsive noise measured in an apartment. In this case, there is the presence of singularity where one of the components collapsed. Thus, with each iteration, the GM density value increased. The parameters were selected using regression analysis and the iteration with the best maximum likelihood estimates was used to model the PDF. It is observed that the two-component GM model gives the best estimate with a correlation coefficient of 0.9877 followed by $q=4$ component model with $R=0.9871$ while the $q=3$ model has the lowest correlation coefficient of $R=0.9828$. Nonetheless, all the R-values are high indicating a strong correlation between the measured data and the GM model densities. From Fig. 7 and 8 which are results from the Post-graduate office, the measured amplitude distributions are observed to have spikes at the peaks. This is due to impulsive noise caused by fluorescent lights, electric kettles, heavy-duty printers and air conditioning units among other appliances which have been confirmed in [2], [17] to contain silicon-controlled rectifiers, rectifier diodes and other power electronic switching devices that produce high levels of impulsive noise. Similar observations can be made in Figs. 9, 10 and 11 which are measurement results from an Apartment and Machines Lab respectively. The results for the highly impulsive category are shown in Fig. 10 and Fig. 11. In this case, the PDF has several peaks with the highest peaks occurring at zero. Considering Fig. 10, the shape of the PDF is more defined in the $q=4$ model followed by $q=3$. At $q=2$, there are two peaks where the second peak does not occur at the mean of the second component distribution.

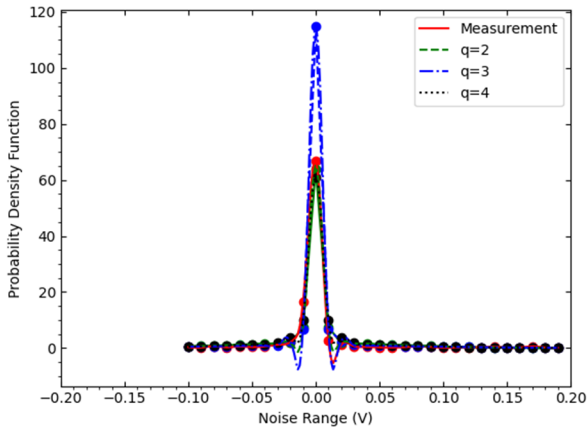


Fig. 9. Medium Impulsive: Apartment

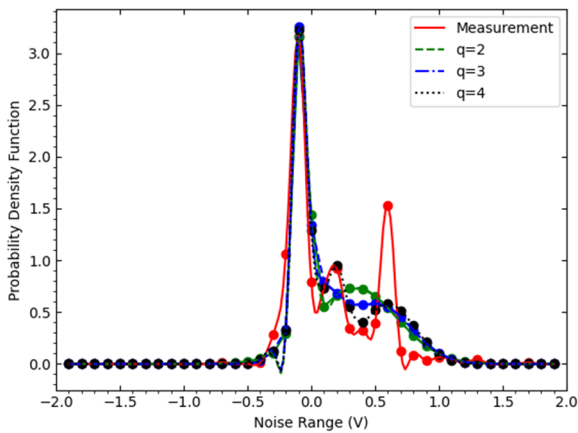


Fig. 10. Highly Impulsive: Measurement 1

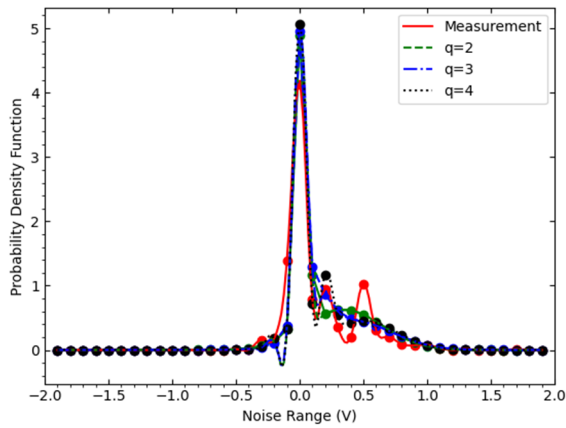


Fig. 11. Highly Impulsive: Measurement 2

In this case, the R-values increase as the number of components in the Gaussian mixture increases as shown in Table III where the highest correlation coefficient is at $q=4$. The RMSE values, on the contrary, decrease with an increase in the number of components where the least RMSE value for measurement 2 is 0.0355. In this category, a higher number of components results in a better fit. This is due to the multi-modal characteristic observed. As Q increases, the shape of the model density distribution becomes more defined and closer to the

measured density. The χ^2 statistical test results for the lowly, medium and highly impulsive categories are summarised in Table IV. It is observed that the χ^2 values for the Computer Lab are less than the critical values for both Measurements 1 and 2. As the number of components constituting the GM model increases, the χ^2 value decreases. Hence, the $q=4$ GM model provides a better fit compared to the $q=3$ and $q=2$ models. In addition, the p-values are greater than 0.05 and therefore conclude that the measured data follows the proposed model. The Post-Graduate office data χ^2 values vary between 7.522-7.9027 and are also seen to be less than the critical value of 36.4150 meaning that the null hypothesis is accepted. Accordingly, the p-values are also greater than 0.05 and can therefore conclude that the measured data is consistent with the GM distribution. It can also be seen that as q increases a better fit is obtained. Although the R and RMSE values of the apartment data indicated a strong correlation for all the three models, the χ^2 values are closer to the critical value where the χ^2 values for the $q=2$ and $q=4$ model are less than the critical value and hence the null hypothesis is accepted.

TABLE III
HIGHLY IMPULSIVE

Machines Lab						
	Measurement 1			Measurement 2		
Model	q=2	q=3	q=4	q=2	q=3	q=4
R	0.9160	0.9282	0.9334	0.9531	0.9571	0.9586
RMSE	0.0427	0.0397	0.0382	0.0378	0.0362	0.0355

TABLE IV
 χ^2 TEST

Computer Lab					
	Model	χ^2	P value	df	Critical Value
Measurement 1	q=2	9.4927	0.6603	12	21.0260
	q=3	7.1429	0.848		
	q=4	6.9873	0.8584		
Measurement 2	q=2	10.9882	0.3588	10	18.3070
	q=3	10.5123	0.3967		
	q=4	5.5325	0.8528		
Post-Graduate Office					
	Model	χ^2	P value	df	Critical Value
Measurement 1	q=2	7.9027	0.9991	24	36.4150
	q=3	7.6701	0.9998		
	q=4	7.5227	0.9998		
Measurement 2	q=2	6.6179	0.9996	24	36.4150
	q=3	7.8061	0.9992		
	q=4	7.7434	0.9993		
Apartment					
	Model	χ^2	P value	df	Critical Value
Measurement 1	q=2	33.8929	0.2851	30	43.7729
	q=3	44.6812	0.0413		
	q=4	30.0886	0.4611		
Machines Lab					
	Model	χ^2	P value	df	Critical Value
Measurement 1	q=2	5.6529	0.9952	17	27.5871
	q=3	4.9463	0.9979		
	q=4	5.2042	0.9971		
Measurement 2	q=2	5.2649	0.9969	17	27.5871
	q=3	4.7111	0.9984		
	q=4	5.0569	0.9976		

However, for $q=3$ the χ^2 value is greater than the critical value of 43.7729. Consequently, the p-value is 0.0413 which is less than 0.05 in which case the null hypothesis is rejected. The significant difference is due to the collapse of one of the component distributions resulting in a sharp rise in the predicted values. At the peak, for example, the proposed model gives a value of 114.75 while the measured PDF value is 66.65. At $q=3$, the proposed model provides a better fit for the measurements carried out in the Machines Lab. This is then followed by the $q=4$ model. In all three models, the χ^2 values are below the critical values and therefore the null hypothesis is true. It can also be observed that as the impulse noise amplitude increases from the low-medium-highly impulsive, the GM model provides a better fit where the average χ^2 value in the low impulsive category is 8.4427. Assuming that there is no singularity case, the medium impulsive χ^2 value is 7.5438 and 5.1394 for the highly impulsive noise category.

VII. Conclusion

In this paper, the amplitude of the impulsive noise has been modelled using a Gaussian mixture where the parameters employed are obtained from measurement data. The impulsive noise has a very unpredictable behaviour in terms of amplitude, burstiness and inter-arrival times. Thus, it is very difficult to have fixed parameters modelling the PDF for different data. The parameters employed in the proposed model are done automatically depending on the data in question.

Therefore, it provides a simplified way of modelling the PDF noise. The GM models are then verified through measurements using the correlation coefficient, RMSE and the χ^2 statistic. It can be seen that for the different noise categories, the accuracy of the predicted PDF increases with an increase in the number of components used to formulate the Gaussian mixture from the correlation coefficient and the RMSE analysis.

However, there is very little difference in the performance of each of the GM at $q=2$, $q=3$ and $q=4$.

Thus, any of the models model can be used to model the PDF of the measured data. All the χ^2 values are less than the respective critical values indicating that the proposed GM model distribution is consistent with measured data except for the $q=3$ component distribution of the measured Apartment results. This shows the effect of singularity on the GM. In order to improve the performance of the model, an alternative parameter estimation method may be employed in future work.

Depending on the parameter under consideration, for example, the shape of the PDF, more components are required in the formulation of the GM model. In low and medium impulsive noise categories, the peaks are not as spread out as those of the high impulsive category. From the measurement results under consideration, it can be seen that the proposed GM model effectively describes the amplitude distribution at different noise levels. Thus, the proposed Gaussian mixture offers a fair estimation of

the impulsive noise amplitude distribution and can be used to evaluate the performance of the PLC channel based on the PLC modulation schemes.

References

- [1] O. Karakuş, E. E. Kuruoğlu, and M. A. Altınkaya, Modelling impulsive noise in indoor powerline communication systems, *Signal, Image and Video Processing*, vol. 14, no. 8, pp. 1655–1661, Nov. 2020. doi: 10.1007/s11760-020-01708-1
- [2] S. O. Awino, T. J. O. Afullo, M. Mosalaosi, and P. O. Akuon, Time Series Analysis of Impulsive Noise in Power Line Communication (PLC) Networks, *SAIEE Africa Research Journal*, vol. 109, no. 4, pp. 237–249, Dec. 2018. doi: 10.23919/SAIEE.2018.8538337
- [3] M. Zimmermann and K. Dostert, Analysis and modeling of impulsive noise in broad-band powerline communications, *IEEE Transactions on Electromagnetic Compatibility*, vol. 44, no. 1, pp. 249–258, 2002. doi: 10.1109/15.990732
- [4] M. Mosalaosi and T. J. O. Afullo, Prediction of asynchronous impulsive noise volatility for indoor powerline communication systems using GARCH models, in *2016 Progress in Electromagnetic Research Symposium (PIERS)*, Aug. 2016, pp. 4876–4880. doi: 10.1109/PIERS.2016.7735782
- [5] Mosalaosi, M., Afullo, T., Broadband Characteristics for Multi-Path Power Line Communication Channels: Indoor Environments, (2016) *International Journal on Communications Antenna and Propagation (IRECAP)*, 6 (4), pp. 244-254. doi: <https://doi.org/10.15866/irecap.v6i4.9797>
- [6] T. Bai et al., Fifty Years of Noise Modeling and Mitigation in Power-Line Communications, *IEEE Communications Surveys & Tutorials*, vol. 23, no. 1, pp. 41–69, 2021. doi: 10.1109/COMST.2020.3033748
- [7] M. Nassar, K. Gulati, Y. Mortazavi, and B. L. Evans, Statistical Modeling of Asynchronous Impulsive Noise in Powerline Communication Networks, in *2011 IEEE Global Telecommunications Conference - GLOBECOM 2011*, Dec. 2011, pp. 1–6. doi: 10.1109/GLOCOM.2011.6134477
- [8] S. Saoudi, T. Derham, T. Ait-Idir, and P. Coupe, A Fast Soft Bit Error Rate Estimation Method, *EURASIP Journal on Wireless Communications and Networking*, vol. 2010, no. 1, p. 372370, Dec. 2010. doi: 10.1155/2010/372370
- [9] J. Dong, *Estimation of bit error rate of any digital communication System*, Université de Bretagne Occidentale, 2013.
- [10] A. M. Tonello, N. A. Letizia, D. Righini, and F. Marcuzzi, Machine Learning Tips and Tricks for Power Line Communications, *IEEE Access*, vol. 7, pp. 82434–82452, 2019. doi: 10.1109/ACCESS.2019.2923321
- [11] S.-I. Seo, Study on Efficient Impulsive Noise Mitigation for Power Line Communication, *International journal of advanced smart convergence*, vol. 8, no. 2, pp. 199–203, 2019. doi: 10.7236/IJASC.2019.8.2.199
- [12] Awino, S., Afullo, T., Mosalaosi, M., Akuon, P., Measurements and Statistical Modelling for Time Behaviour of Power Line Communication Impulsive Noise, (2019) *International Journal on Communications Antenna and Propagation (IRECAP)*, 9 (4), pp. 236-246. doi: <https://doi.org/10.15866/irecap.v9i4.16094>
- [13] M. O. Asiyu and T. J. O. Afullo, Analysis of Bursty Impulsive Noise in Low-Voltage Indoor Power Line Communication Channels: Local Scaling Behaviour, *SAIEE Africa Research Journal*, vol. 108, no. 3, pp. 98–107, Sep. 2017. doi: 10.23919/SAIEE.2017.8531521
- [14] M. Mosalaosi, *Characterization and modeling of the channel and noise for broadband indoor Power Line Communication (PLC) networks*, Ph.D. dissertation, University of KwaZulu-Natal, Durban, South Africa, 2016.
- [15] A. Emlh, A. S. de Beer, H. C. Ferreira, and A. J. H. Vinck, Noise

- detection on the low voltage network PLC channel for direct and indirect connections, in *MELECON 2014 - 2014 17th IEEE Mediterranean Electrotechnical Conference*, Apr. 2014, pp. 203–207.
doi: 10.1109/MELCON.2014.6820532
- [16] A. Acakpovi, H. Mohammed, N. Nwulu, F.-X. N. Fifatin, T. C. Nounangnonhou, and R. Abubakar, Evaluation of Noise Effects on Power Line Communication in a Narrow and Wide Band Frequency Spectrum: A Case Study of Electricity Distribution Network of Ghana, in *2019 International Conference on Computing, Computational Modelling and Applications (ICCOMA)*, Mar. 2019, pp. 27–276.
doi: 10.1109/ICCOMA.2019.00012
- [17] H. Meng, Y. L. Guan, and S. Chen, Modeling and Analysis of Noise Effects on Broadband Power-Line Communications, *IEEE Transactions on Power Delivery*, vol. 20, no. 2, pp. 630–637, Apr. 2005.
doi: 10.1109/TPWRD.2005.844349
- [18] S. O. Awino, T. J. O. Afullo, M. Mosalaosi, and P. O. Akuon, Empirical Identification of Narrowband Interference in Broadband PLC Networks at the Receiver, in *2018 Progress in Electromagnetics Research Symposium (PIERS-Toyama)*, Aug. 2018, pp. 2160–2164.
doi: 10.23919/PIERS.2018.8597885
- [19] J. Yin, X. Zhu, and Y. Huang, 3D Markov Chain Based Narrowband Interference Model for In-Home Broadband Power Line Communication, in *2016 IEEE Global Communications Conference (GLOBECOM)*, Dec. 2016, pp. 1–6.
doi: 10.1109/GLOCOM.2016.7841485
- [20] A. Ohno, Osamu and Katayama, Masaaki and Yamazato, Takaya and Ogawa, A simple model of cyclostationary power-line noise for communication systems, in *International Symposium on Power Line Communications and Its Applications (ISPLC)*, 1998, pp. 115–122.
- [21] M. O. Asiyo and T. J. Afullo, Prediction of long-range dependence in cyclostationary noise in low-voltage PLC networks, in *2016 Progress in Electromagnetic Research Symposium (PIERS)*, Aug. 2016, pp. 4954–4958.
doi: 10.1109/PIERS.2016.7735807
- [22] M. Mosalaosi and T. Afullo, Parameter estimation for linear regression models in powerline communication systems noise using Generalized Method of Moments (GMM), in *Progress in Electromagnetic Research Symposium (PIERS)*, 2016, pp. 4858–4862.
- [23] H. Oh, D. Seo, and H. Nam, Design of a Test for Detecting the Presence of Impulsive Noise, *Sensors*, vol. 20, no. 24, p. 7135, Dec. 2020.
doi: 10.3390/s20247135
- [24] Abraham M. Nyete, 2017, A Novel Technique for the Modeling of Power Line Noise for PLC Low Voltage Applications, *International Journal of Engineering Research & Technology (IJERT)* Volume 06, Issue 04 (April 2017),
- [25] T. Shongwe, A. J. H. Vinck, and H. C. Ferreira, A Study on Impulse Noise and Its Models, *SAIEE Africa Research Journal*, vol. 106, no. 3, pp. 119–131, Sep. 2015.
doi: 10.23919/SAIEE.2015.8531938
- [26] C. L. Brown and A. M. Zoubir, A nonparametric approach to signal detection in impulsive interference, *IEEE Transactions on Signal Processing*, vol. 48, no. 9, pp. 2665–2669, 2000.
doi: 10.1109/78.863074
- [27] G. Laguna-Sanchez and M. Lopez-Guerrero, On the Use of Alpha-Stable Distributions in Noise Modeling for PLC, *IEEE Transactions on Power Delivery*, vol. 30, no. 4, pp. 1863–1870, Aug. 2015.
doi: 10.1109/TPWRD.2015.2390134
- [28] D. Middleton, Statistical-Physical Models of Electromagnetic Interference, *IEEE Transactions on Electromagnetic Compatibility*, vol. EMC-19, no. 3, pp. 106–127, Aug. 1977.
doi: 10.1109/TEMC.1977.303527
- [29] B. S. Sushma, R. Roopesh, S. Gurugopinath, and R. Muralishankar, Performance Characterization of Broadband Powerline Communication for Internet-of-Things, in *2019 International Conference on Wireless Communications Signal Processing and Networking (WiSPNET)*, Mar. 2019, pp. 146–151.
doi: 10.1109/WiSPNET.2019.9032857
- [30] H. A. Suraweera and J. Armstrong, Noise bucket effect for impulsive noise in OFDM, *Electronics Letters*, vol. 40, no. 18, p. 1156, 2004.
doi: 10.1049/el:20045825
- [31] G. Ndo, F. Labeau, and M. Kassouf, A Markov-Middleton Model for Bursty Impulsive Noise: Modeling and Receiver Design, *IEEE Transactions on Power Delivery*, vol. 28, no. 4, pp. 2317–2325, Oct. 2013.
doi: 10.1109/TPWRD.2013.2273942
- [32] S. P. Herath, N. H. Tran, and T. Le-Ngoc, On optimal input distribution and capacity limit of Bernoulli-Gaussian impulsive noise channels, in *2012 IEEE International Conference on Communications (ICC)*, Jun. 2012, pp. 3429–3433.
doi: 10.1109/ICC.2012.6364379
- [33] T. Guzel, E. Ustunel, H. B. Celebi, H. Delic, and K. Mihcak, Noise Modeling and OFDM Receiver Design in Power-Line Communication, *IEEE Transactions on Power Delivery*, vol. 26, no. 4, pp. 2735–2742, Oct. 2011.
doi: 10.1109/TPWRD.2011.2164814
- [34] F. Gianaroli, F. Pancaldi, and G. M. Vitetta, The Impact of Statistical Noise Modeling on the Error-Rate Performance of OFDM Power-Line Communications, *IEEE Transactions on Power Delivery*, vol. 29, no. 6, pp. 2622–2630, Dec. 2014.
doi: 10.1109/TPWRD.2014.2311167
- [35] S. O. Awino, T. J. O. Afullo, M. Mosalaosi, and P. O. Akuon, GMM Estimation and BER of Bursty Impulsive Noise in Low-voltage PLC Networks, in *2019 Photonics & Electromagnetics Research Symposium - Spring (PIERS-Spring)*, Jun. 2019, pp. 1828–1834.
doi: 10.1109/PIERS-Spring46901.2019.9017860
- [36] T. Samakande, T. Shongwe, A. S. de Beer, and H. C. Ferreira, The effect of coupling circuits on impulsive noise in power line communication, in *2018 IEEE International Symposium on Power Line Communications and its Applications (ISPLC)*, Apr. 2018, pp. 1–5.
doi: 10.1109/ISPLC.2018.8360232
- [37] M. P. Deisenroth, A. A. Faisal, and C. S. Ong, *Mathematics for machine learning*. Cambridge University Press, 2020.
- [38] N. M. Bishop, Christopher M and Nasrabadi, *Pattern recognition and machine learning*, Vol. 4, No. Springer, 2006.
- [39] B. Ghogh, A. Ghogh, M. Crowley, and F. Karray, Fitting a mixture distribution to data: tutorial, *arXiv preprint arXiv:1901.06708*, 2019.
- [40] A. Emlah, A. S. de Beer, H. C. Ferreira, and A. J. H. Vinck, The influence of fluorescent lamps with electronic ballast on the low voltage PLC network, in *2014 IEEE 8th International Power Engineering and Optimization Conference (PEOCO2014)*, Mar. 2014, pp. 276–280.
doi: 10.1109/PEOCO.2014.6814439

Authors' information

Discipline of Electrical, Electronic and Computer Engineering, The University of KwaZulu-Natal, Durban, South Africa.



Florence Chelangat received her BEng. degree (Hons.) in electrical and electronic engineering from the Technical University of Kenya, Nairobi, Kenya, in 2014 and an MScEng in electronic engineering at the University of KwaZulu-Natal, Durban, South Africa in 2019. She is currently pursuing a PhD in electronic engineering at the University of KwaZulu-Natal.

Her research interest is in powerline communications and microwaves. Ms Florence Chelangat is a student member of IEEE.



Thomas J. O. Afullo is currently the Director of Telkom Centre for Radio Access & Rural Technologies (CRART) and a Professor in the Discipline of Electrical, Electronic & Computer Engineering at the University of KwaZulu-Natal, Durban, South Africa. The former Discipline Academic Leader attained his Bachelor's degree in electrical and electronic engineering (Hons)

from the University of Nairobi in 1979, MSEE from the University of West Virginia, USA in 1983 and PhD in electrical engineering from Vrije Universiteit (VUB), Belgium in the year 1989. His research interests include Radioclimatological Modelling, Microwave & Antenna Engineering and RF propagation modelling at millimetre & microwaves, powerline communications and free space optics. Prof. Afullo is a registered Professional Engineer in South Africa and Kenya, a Fellow of the South African Institute of Electrical Engineers (FSAIEE), a senior member of IEEE and a member of Eta Kappa Nu (MHKN).